Sparse Aperture Masking with SPHERE

Anthony C. Cheetham[a], Julien Girard[b], Sylvestre Lacour[c], Guillaume Schworer[c], Xavier Haubois[b], and Jean-Luc Beuzit[d]

[a]Observatoire de Genève, Université de Genève, 51 chemin des Maillettes, 1290, Versoix, Switzerland
[b]European Southern Observatory, Alonso de Cordova 3107, Casilla 19001 Vitacura, Santiago 19, Chile
[c]LESIA/Observatoire de Paris, PSL, CNRS, UPMC, Universite Paris Diderot, 5 place Jules Janssen, F-92195 Meudon, France
[d]Université Grenoble Alpes, CNRS, IPAG, 38000 Grenoble, France

ABSTRACT

Sparse Aperture Masking (SAM) has recently been commissioned on SPHERE, the VLTs new adaptive optics high resolution imager. SAM extends the capabilities of SPHERE by providing high contrast measurements at and beyond the traditional diffraction limit. SAM can be used in conjunction with each of the SPHERE modules (IRDIS, IFS and ZIMPOL), allowing dual band imaging in the visible and near-infrared, near-infrared integral field spectroscopy, and polarized differential imaging in the visible and near-infrared. In this paper we report information relevant for observers as well as some commissioning observations.

Keywords: Interferometry, High Resolution Imaging

1. INTRODUCTION

Sparse Aperture Masking (SAM) has established itself as one of the most successful techniques for obtaining high contrast measurements at small angular separations. By trading the achievable contrast to explore the smallest possible separations it has found a multitude of uses, such as the study of stellar and substellar multiplicity in nearby star-forming regions,[1–3] the discovery of low mass companions to young stars,[4,5] the study of stellar winds of evolved stars,[6,7] and the study of active galactic nuclei.[8]

The goal of SAM is to turn the telescope into a sparse interferometric array, which provides distinct advantages and disadvantages compared to other high resolution imaging techniques. This is achieved through the use of an opaque mask that turns the telescope aperture into an array of smaller circular subapertures, which changes the instrument PSF into an interference pattern.

The primary advantage of observing with SAM is the use of robust observables such as closure phase (and kernel phase[9]) that are insensitive to residual wavefront errors, allowing high contrasts to be reached at angular separations where these errors typically dominate. Being an interferometric method, SAM allows measurements to be made beyond the Rayleigh diffraction limit, down to separations smaller than $0.5\lambda/D$. However, the field of view of SAM observations is typically limited to $\sim 5\lambda/D$ and the contrasts achieved are not comparable to those obtained at larger separations through other techniques (such as coronagraphy). For these reasons, it has found a niche as a useful technique for detecting structures with moderate contrasts at or close to the diffraction limit.

The combination of SAM with adaptive optics (AO) began has been highly successful with the Keck-NIRC2 and VLT-NACO instruments.[10,11] While using SAM on older instruments such as Keck-NIRC[12] required extremely short exposure times to freeze the effects of atmospheric turbulence, AO has allowed much longer exposure times and correspondingly fainter stars to be observed.

Further author information: (Send correspondence to A.C.C)
A.C.C.: E-mail: anthony.cheetham@unige.ch

Optical and Infrared Interferometry and Imaging V, edited by Fabien Malbet, Michelle J. Creech-Eakman, Peter G. Tuthill, Proc. of SPIE Vol. 9907, 99072T
 · doi: 10.1117/12.2231983

While closure phases are robust to phase errors, they typically suffer from systematics caused by a variety of factors. The main culprits include wavefront error on spatial scales smaller than the mask holes, time-varying wavefront error during an exposure, and the wavelength-dependent nature of wavefront error coupled with wide filter bandpasses. To correct for these systematics, calibrator stars are observed in the same observing sequence and the measured closure phases are subtracted from those of the target. At present, long SAM observations aiming to reach the highest possible contrast are typically limited by this subtraction, since the systematics themselves can change with time and when observing different targets.

With the introduction of Extreme AO systems such as SPHERE[13] and GPI,[14] the superior wavefront correction compared to previous generation AO systems is also advantageous to SAM, reducing both the magnitude and variation of the systematic errors. In addition, both SPHERE and GPI have integral field spectrographs, allowing for the combination of SAM with low resolution spectroscopy. Both instruments have aperture masks installed, and recent results from GPI showed a substantial improvement in obtainable contrast and astrometric accuracy compared to previous generation instruments.[15]

Here we present a summary of observing modes and information relevant for observing using SAM with SPHERE.

2. SPHERE APERTURE MASKING

The Spectro-Polarimetric High-contrast REsearch (SPHERE) instrument consists of 3 modules: a near-IR imager and polarimeter (IRDIS), a near-IR integral field spectrograph (IFS) and a visible light imager and polarimeter (ZIMPOL). All three modules were designed primarily with the purpose of using high contrast imaging to directly detect exoplanets and improve our understanding of the planet formation process.[13]

2.1 Aperture Masks

Three aperture masks are installed in SPHERE. All are of the same basic 7-hole design also deployed on NACO,[11] but are located within the different instrument modules such that SAM can be used with IRDIS, IFS and ZIMPOL. The general layout of the mask design is shown in Figure 1. The rotation and size of each mask varies between the instrument modules. The coordinates of each mask hole for each module is listed in Table 1, expressed with reference to the VLT primary mirror size and projected onto the detector coordinates. However, we caution that the scaling and rotation were measured from a single epoch in July 2015 and are provided as a guide only; the hole positions should be updated or checked for each new set of observations.

The design of these masks requires balancing several competing factors. The 7 hole design employed in SPHERE is optimized for detecting point sources around faint targets. The small number of mask holes trades a modest Fourier coverage for larger holes which maximize the throughput. However, this does not preclude its use for other purposes.

Figure 2 shows four on-sky images taken with the different modules of SPHERE in imaging mode, to illustrate the instrument's range of capabilities. Even with long (10 s) exposures in R band on a moderately bright (R=8) target, the extreme AO system maintains enough wavefront stability to maintain fringe contrast and allow high contrast measurements. In comparison, short exposure images at K band show the exquisite wavefront correction at longer wavelengths that leads to highly stable closure phase and visibility measurements with SPHERE.

2.2 Observing Modes

SAM can be used with any of the imaging modes of SPHERE. These include IRDIS+IFS simultaneously (called IRDIFS mode), IRDIS classical imaging mode, IRDIS dual band imaging, IRDIS dual polarization imaging, ZIMPOL classical imaging, and ZIMPOL polarimetry. IRDIS long slit spectroscopy mode is not supported. Any of the filters listed in the SPHERE manual can be used. ZIMPOL operates at visible wavelengths between 550 nm and 1 μm, while IRDIS operates between 1 and 2.3 μm.[13] IFS provides 39 wavelength channels between Y and J band with an average spectral resolving power of 55, but can also be used in extended wavelength mode between Y and H band with an average spectral resolution of 35.

SAM observing uses pupil tracking mode, which freezes the orientation of the telescope pupil with respect to the detector while allowing the sky to rotate during an observation. This ensures that the mask holes sample the

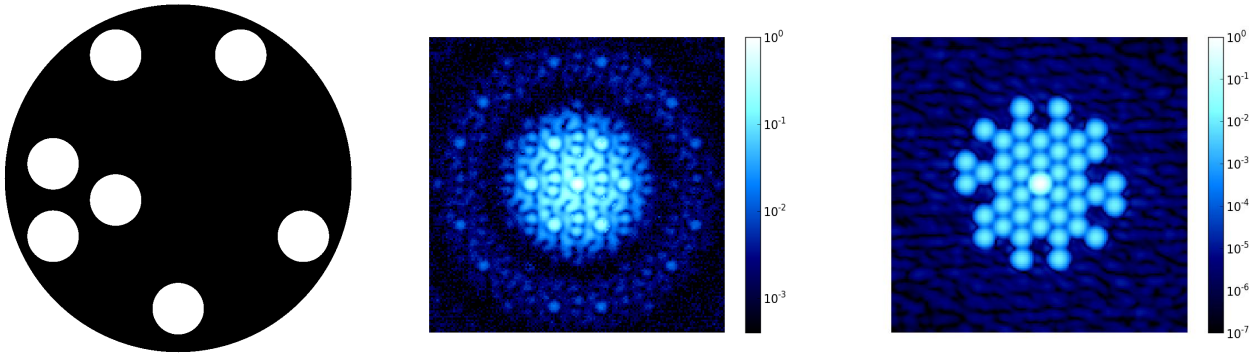

Figure 1. **Left**: Diagram of the 7 hole aperture mask design used by each of the SPHERE instrument modules, overlaid on the VLT primary mirror. The SAM mask located in each module is a scaled and rotated version of this design. This 7 hole design provies a relatively high throughput and modest Fourier coverage. **Middle**: A short exposure on-sky K-band image taken with the 7 hole mask with the IRDIS camera. Each pair of holes in the SAM mask produces a set of interference fringes. For the 7 hole mask, there are 21 pairs (called baselines). The mask design ensures that the vector separating each pair of holes is unique, and hence each set of fringes has a unique frequency and direction. The final PSF is a combination of the Airy pattern produced by a single hole modulated by the interference fringes. **Right**: Taking the Fourier transform of the previous image separates the image into its component frequencies. The baselines are well separated, allowing their amplitude and frequency to be measured easily. The phases can be turned into closure phases by summing the phase from baselines that share the same three mask holes.

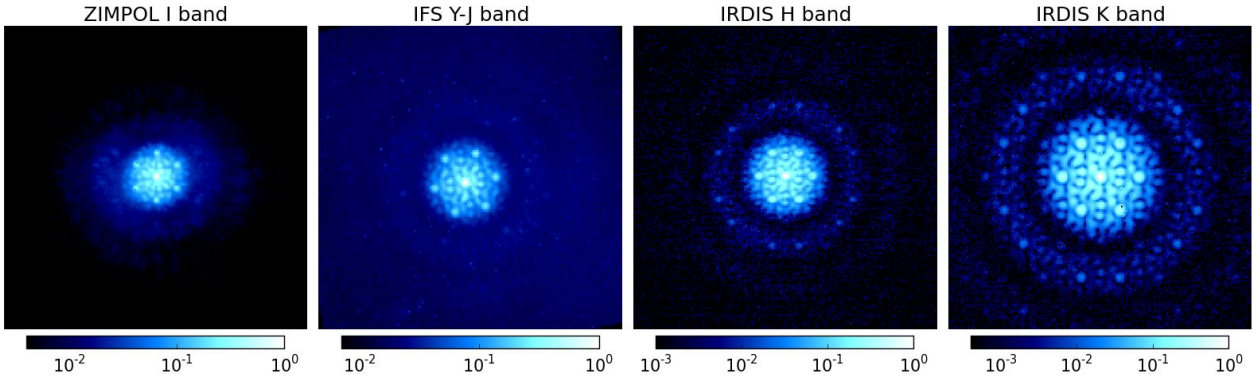

Figure 2. On-sky PSFs taken with the different modules of SPHERE during the commissioning night in July 2015. From left to right, the PSFs show a 10 second exposure in R band with ZIMPOL on a faint target, an IFS wavelength slice from between Y and H bands from a 4s integration, a 0.84s image taken with the H2 filter using IRDIS, and a short exposure 0.22s image from IRDIS using the NB_CO filter.

Table 1. SPHERE aperture mask hole positions in July 2015

IFS		IRDIS		ZIMPOL	
X (m)	Y (m)	X (m)	Y (m)	X (m)	Y (m)
-2.07	2.71	-1.46	2.87	3.06	1.50
0.98	3.27	1.46	2.87	3.02	-1.60
-3.11	-0.20	-2.92	0.34	0.41	3.09
-1.43	-0.81	-1.46	-0.51	-0.51	1.56
-2.79	-1.96	-2.92	-1.35	-1.38	3.12
3.30	-0.85	2.92	-1.35	-1.48	-3.07
0.58	-3.17	0.00	-3.04	-3.22	0.05

same part of the wavefront during an observing sequence so that instrument systematics are kept as consistent as possible, and that the mask holes do not cross the telescope spiders.

2.3 Exposure Times

The SAM masks block around 85% of the pupil area. Combining this factor with the shape of the SAM PSF, this results in a factor 40 reduction in the peak flux compared to the unocculted PSF. The exposure times and peak fluxes estimated for the non-coronagraphic imaging modes can be converted to SAM exposure times using this factor.

2.4 PSF Calibration

As an interferometric mode, SAM requires the regular observation of calibrator stars to measure instrument systematics. This is usually achieved by observing known unresolved point sources with similar visible and infrared magnitudes at regular intervals during an observing sequence. These targets should also be chosen to have similar airmass and location in the sky to ensure similar observing conditions and optimal calibration of systematics.

To further improve the calibration, several visits between target and calibrator are usually made. This will help to explore the instrument systematics, as well as their temporal evolution during a long sequence of observations. In addition, such an observing strategy maximises the sky rotation between observations and hence the Fourier coverage, providing better reconstruction of any detected structures.

3. CONCLUSIONS

The Sparse Aperture Masking mode of SPHERE turns the single-aperture VLT primary mirror into a sparse interferometric array, giving access to robust observables that allow high contrast measurements to be made at the diffraction limit. This is achieved primarily through the use of the closure phase observable that is robust to wavefront errors and non-common path error, factors that typically limit the achievable contrast of other techniques at close separations.

SAM can be used in conjunction with any of the imaging or polarimetric modes of SPHERE. This allows imaging at wavelengths ranging from 550 nm to 2.3 μm, polarimetric imaging across the same wavelength range, and integral field spectroscopy between Y-J or Y-H bands. The 7 hole mask design used with SPHERE is designed primarily for detecting faint companions at the diffraction limit, trading Fourier-coverage for throughput.

The combination of SAM with SPHERE's extreme AO system and multitude of observing modes is an exciting prospect for a range of science cases that benefit from high contrast imaging or polarimetry at the diffraction limit.

ACKNOWLEDGMENTS

This work has been carried out within the framework of the National Centre for Competence in Research "PlanetS" supported by the Swiss National Science Foundation (SNSF). Based on observations collected at the European Organisation for Astronomical Research in the Southern Hemisphere under ESO programme 60.A-9800(S).

REFERENCES

[1] Kraus, A. L., Ireland, M. J., Martinache, F., and Lloyd, J. P., "Mapping the Shores of the Brown Dwarf Desert. I. Upper Scorpius," *ApJ* **679**, 762–782 (May 2008).

[2] Hinkley, S., Kraus, A. L., Ireland, M. J., Cheetham, A., Carpenter, J. M., Tuthill, P., Lacour, S., Evans, T. M., and Haubois, X., "Discovery of Seven Companions to Intermediate-mass Stars with Extreme Mass Ratios in the Scorpius-Centaurus Association," *ApJL* **806**, L9 (June 2015).

[3] Cheetham, A. C., Kraus, A. L., Ireland, M. J., Cieza, L., Rizzuto, A. C., and Tuthill, P. G., "Mapping the Shores of the Brown Dwarf Desert. IV. Ophiuchus," *ApJ* **813**, 83 (Nov. 2015).

[4] Kraus, A. L. and Ireland, M. J., "Lkca 15: A young exoplanet caught at formation?," *ApJ* **745**(1), 5 (2012).

[5] Biller, B., Lacour, S., Juhász, A., Benisty, M., Chauvin, G., Olofsson, J., Pott, J.-U., Müller, A., Sicilia-Aguilar, A., Bonnefoy, M., Tuthill, P., Thebault, P., Henning, T., and Crida, A., "A Likely Close-in Low-mass Stellar Companion to the Transitional Disk Star HD 142527," *ApJL* **753**, L38 (July 2012).

[6] Monnier, J. D., Tuthill, P. G., Lopez, B., Cruzalebes, P., Danchi, W. C., and Haniff, C. A., "The Last Gasps of VY Canis Majoris: Aperture Synthesis and Adaptive Optics Imagery," *ApJ* **512**, 351–361 (Feb. 1999).

[7] Norris, B. R. M., Tuthill, P. G., Ireland, M. J., Lacour, S., Zijlstra, A. A., Lykou, F., Evans, T. M., Stewart, P., and Bedding, T. R., "A close halo of large transparent grains around extreme red giant stars," *Nature* **484**, 220–222 (Apr. 2012).

[8] Ford, K. E. S., McKernan, B., Sivaramakrishnan, A., Martel, A. R., Koekemoer, A., Lafrenière, D., and Parmentier, S., "Active Galactic Nucleus and Quasar Science with Aperture Masking Interferometry on the James Webb Space Telescope," *ApJ* **783**, 73 (Mar. 2014).

[9] Martinache, F., "Kernel Phase in Fizeau Interferometry," *ApJ* **724**, 464–469 (Nov. 2010).

[10] Tuthill, P., Lloyd, J., Ireland, M., Martinache, F., Monnier, J., Woodruff, H., ten Brummelaar, T., Turner, N., and Townes, C., "Sparse-aperture adaptive optics," *Proc. SPIE* **6272**, 103 (June 2006).

[11] Lacour, S., Tuthill, P., Amico, P., Ireland, M., Ehrenreich, D., Huélamo, N., and Lagrange, A.-M., "Sparse aperture masking at the VLT. I. Faint companion detection limits for the two debris disk stars HD 92945 and HD 141569," *A&A* **532**, A72 (Aug. 2011).

[12] Tuthill, P. G., Monnier, J. D., Danchi, W. C., Wishnow, E. H., and Haniff, C. A., "Michelson Interferometry with the Keck I Telescope," *PASP* **112**, 555–565 (Apr. 2000).

[13] Beuzit, J.-L., Feldt, M., Dohlen, K., Mouillet, D., Puget, P., Wildi, F., Abe, L., Antichi, J., Baruffolo, A., Baudoz, P., Boccaletti, A., Carbillet, M., Charton, J., Claudi, R., Downing, M., Fabron, C., Feautrier, P., Fedrigo, E., Fusco, T., Gach, J.-L., Gratton, R., Henning, T., Hubin, N., Joos, F., Kasper, M., Langlois, M., Lenzen, R., Moutou, C., Pavlov, A., Petit, C., Pragt, J., Rabou, P., Rigal, F., Roelfsema, R., Rousset, G., Saisse, M., Schmid, H.-M., Stadler, E., Thalmann, C., Turatto, M., Udry, S., Vakili, F., and Waters, R., "SPHERE: a 'Planet Finder' instrument for the VLT," in [*Proceedings of the SPIE*], **7014** (July 2008).

[14] Macintosh, B. A., Graham, J. R., Palmer, D. W., Doyon, R., Dunn, J., Gavel, D. T., Larkin, J., Oppenheimer, B., Saddlemyer, L., Sivaramakrishnan, A., Wallace, J. K., Bauman, B., Erickson, D. A., Marois, C., Poyneer, L. A., and Soummer, R., "The Gemini Planet Imager: from science to design to construction," in [*Proceedings of the SPIE*], **7015** (July 2008).

[15] Greenbaum, A. Z., Cheetham, A., Sivaramakrishnan, A., Tuthill, P., Norris, B., Pueyo, L., Sadakuni, N., Rantakyrö, F., Hibon, P., Goodsell, S., Hartung, M., Serio, A., Cardwell, A., Poyneer, L., Macintosh, B., Savransky, D., Perrin, M. D., Wolff, S., Ingraham, P., Thomas, S., and with the GPI team, "Gemini Planet imager Observational Calibrations X: Non-Redundant Masking on GPI," *ArXiv e-prints* (July 2014).